Electronic Supplementary Material (ESI) for Green Chemistry.

Supporting Information

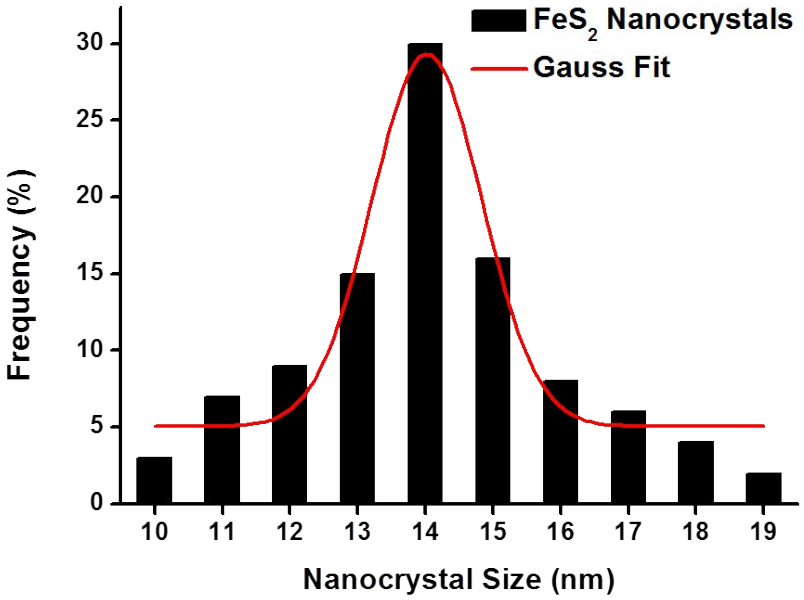

Figure S1. Histogram of size distribution of FeS_2 and Gaussian fitting.

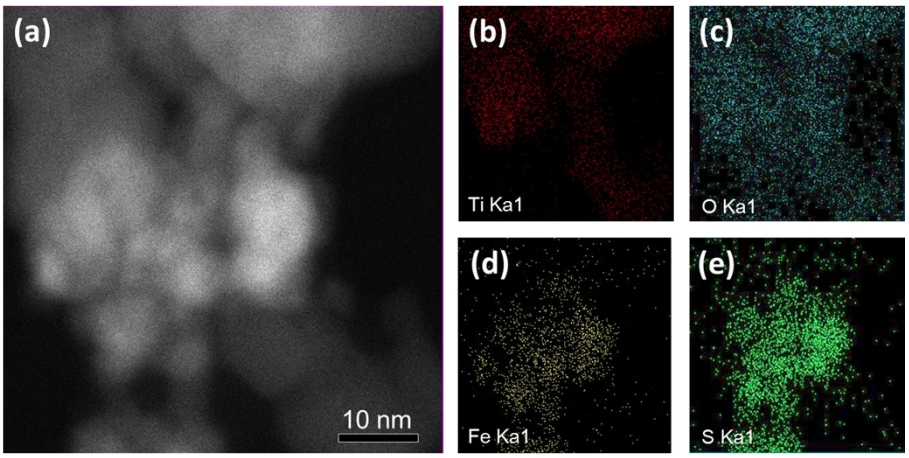

Figure S2. (a) HAADF-STEM images of FeS_2-TiO_2 heterostructures and their selected EDS mapping of (b) Ti, (c) O, (d) Fe, and (e) S. As shown in Figure S2, the elements of Ti, O, Fe and S can be clearly observed in the FeS_2-TiO_2 heterostructure, which results further suggested the successful conjugation of FeS_2 NCs and TiO_2 NPs to form the FeS_2-TiO_2 heterostructures

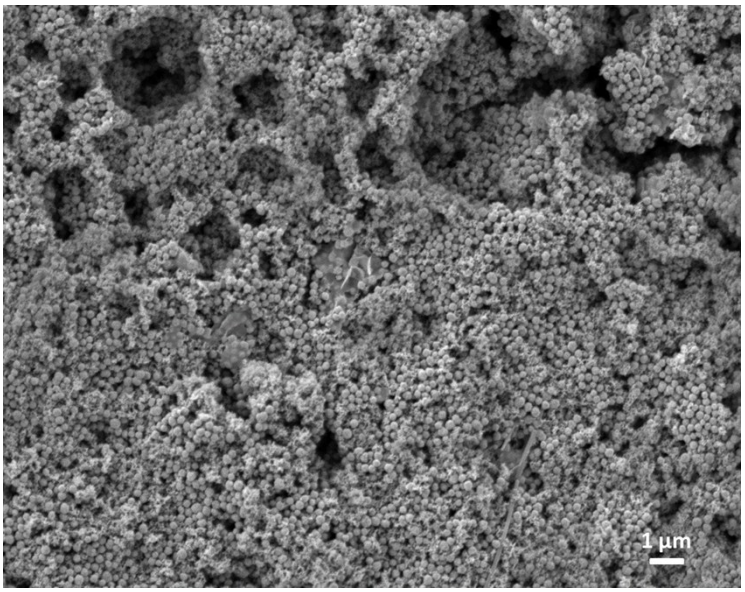

Figure S3. SEM image of FeS_2-TiO_2 heterostructures.

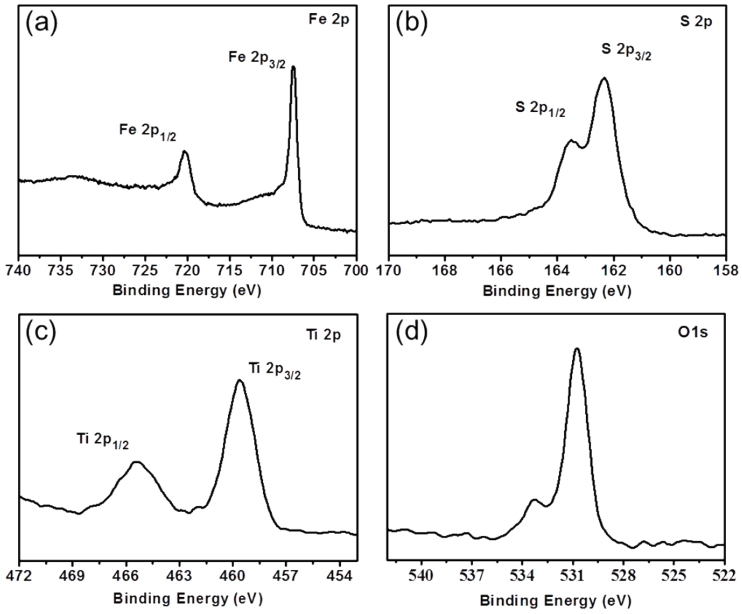

Figure S4. X-ray photoemission spectra of FeS_2-TiO_2 heterostructures. (a) In the XPS Fe(2p) spectra, characteristic peaks of Fe($2P_{1/2}$) and Fe($2p_{3/2}$) were respectively detected at binding energies of 707.5 and 720.3 eV due to Fe_2^+ of FeS_2 structure. (b) The binding energies of S($2p_{1/2}$) at 163.5 eV and S($2p_{3/2}$) at 162.3 eV were attributed to S_2^{2-} of FeS_2, indicating that a pyrite structure of FeS_2 was formed in FeS_2-TiO_2 heterostructures. (c) The XPS spectra of Ti ($2p_{1/2}$) at binding energy 465.4 eV and Ti

($2p_{3/2}$) at binding energy 459.6 eV revealed Ti^{4+} of TiO_2 in FeS_2-TiO_2 heterostructures. (d) For the XPS spectra of O(1s), the main peak at 530.8 eV was ascribed to lattice oxygen in TiO_2, while the binding energy at 533.3 eV could be associated to surface hydroxyl groups.

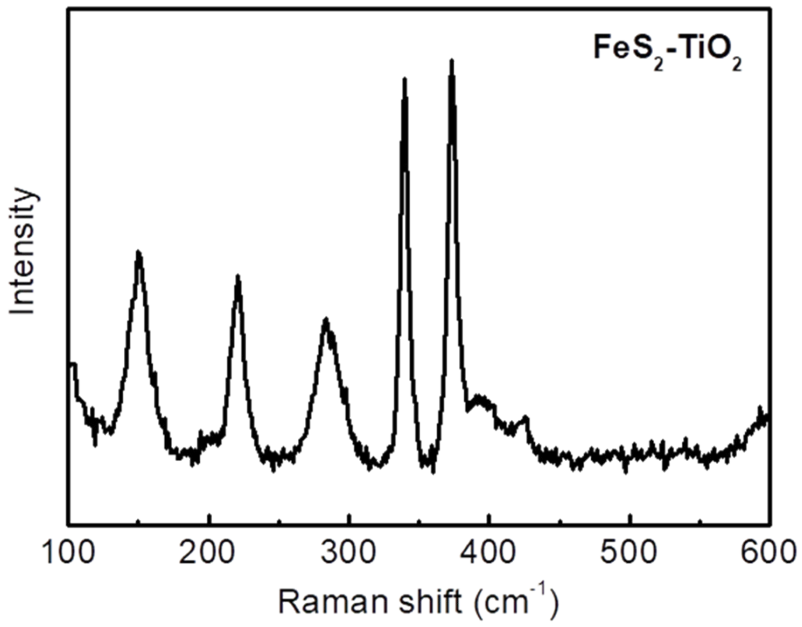

Figure S5. Raman spectra of FeS_2-TiO_2 heterostructures. Raman spectroscopy was performed to probe the surface structure of FeS_2-TiO_2 heterostructures. The Raman spectrum showed three peaks at 343, 379, and 430 cm^{-1}, which are the characteristic active modes for pyrite corresponding to the S_2 vibration (E_g), S-S in-phase stretch (A_g), and coupled vibration and stretch (T_g) modes, respectively. The peak at 150 cm^{-1} is originated from P25 TiO_2. Besides, there is a few FeS phase (presence of Raman peaks at 214 and 282 cm^{-1}) observed in the heterostructures. Some FeS phases in the FeS_2 NCs could be caused by the sulfur deficiency on the surface of FeS_2 NCs.

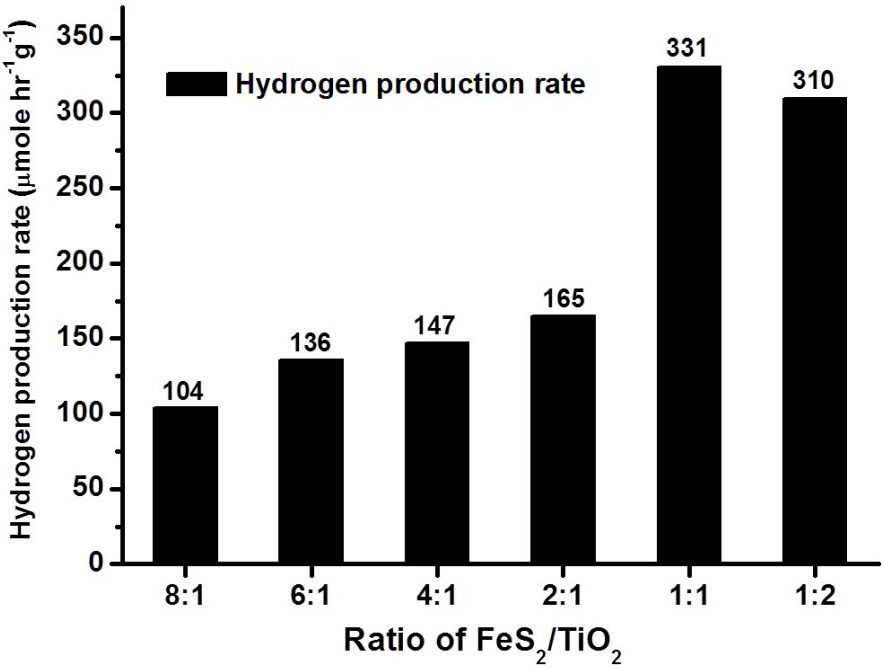

Figure S6. Hydrogen production rates of FeS_2-TiO_2 heterostructures at different weight ratios of FeS_2 to TiO_2.

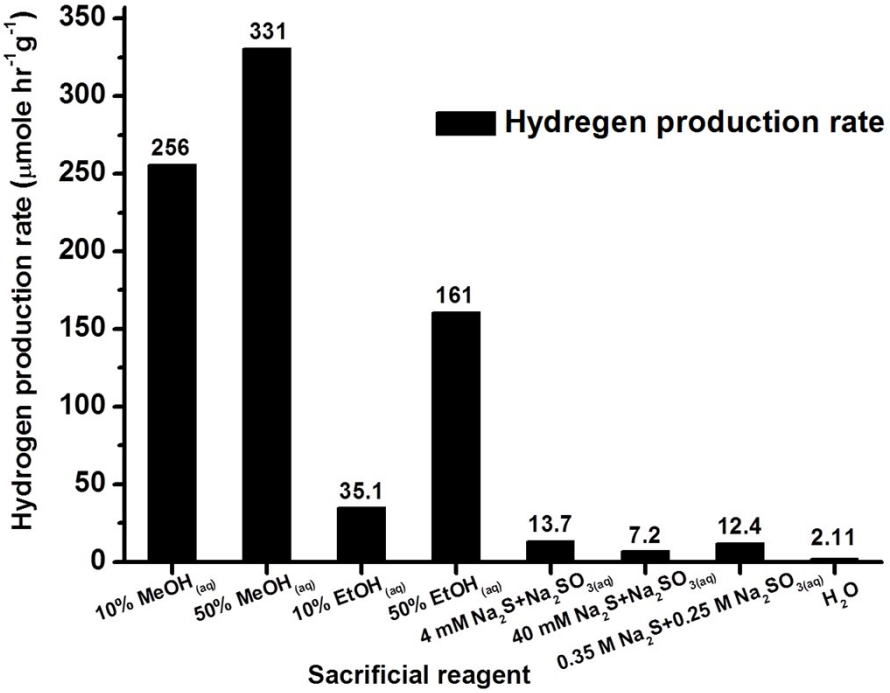

Figure S7. Hydrogen production rates of FeS_2-TiO_2 heterostructures with different sacrificial reagents.

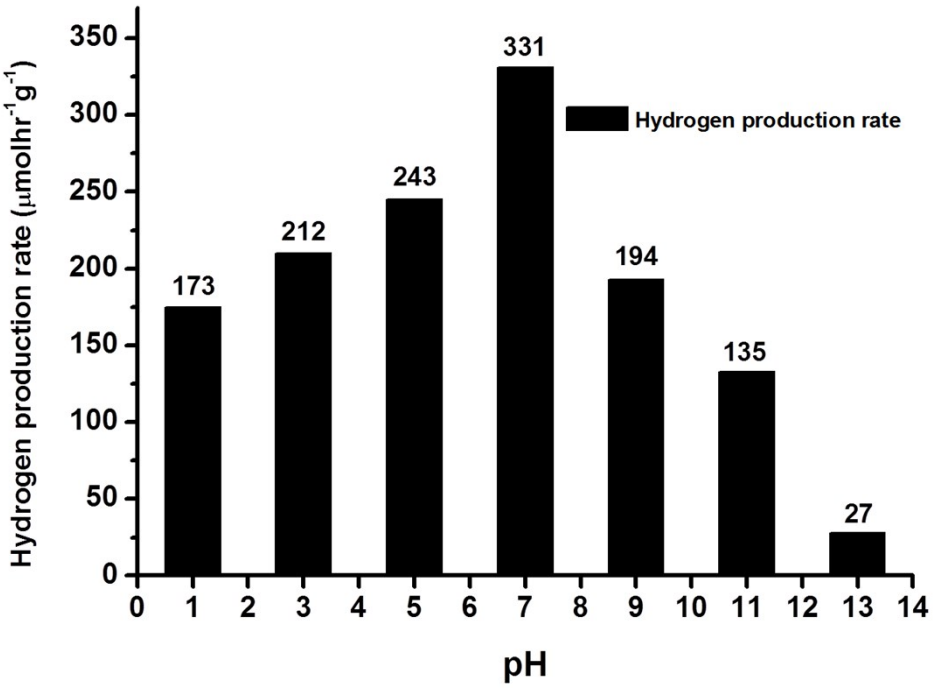

Figure S8. Photocatalytic hydrogen production rates of FeS_2-TiO_2 heterostructures in different pH aqueous solution with 50% methanol as a sacrificial agent.

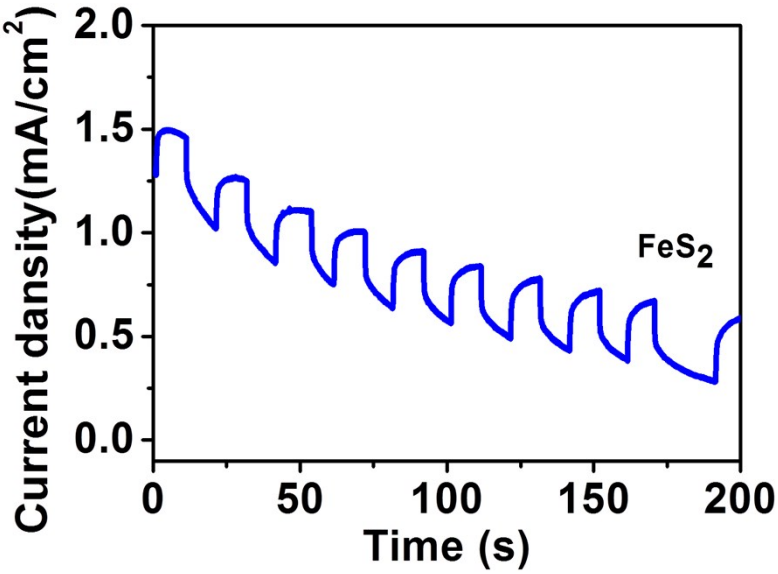

Figure S9. The current-time (*i-t*) characteristics of the pure FeS_2 under the on/off cycles of the NIR laser (808 nm) illumination at a constant bias of 0.1V. The materials was placed as on the FTO substrate as an anode electrode.